Controlled Interfacial Phenomena for Extended Battery Life

Perla B. Balbuena

Texas A&M University

June 1-4, 2020

Project ID #: bat449

Overview

Timeline

- Start date: October 1, 2017
- End date: March 31, 2021
- Percent complete: 70%

Budget

- Total funding: $1,333,380
  – DOE share: $1,200,000
  – Contractor share: $133,380
- Funding received
  – FY19: $343,000
  – FY20: $343,000

Barriers

- Barriers/targets addressed
  - Loss of available capacity
  - Materials degradation during cycling
  - Lifetime of the cell

Partners

- Interactions/collaborations
  – J. Seminario (TAMU Co-PI)
  – J. Zhang, X. Cao (PNNL collaborators)

- Project lead: TAMU

Relevance

Impact

Achieving an energy density ≥500 Wh/Kg with a life of ≥1,000 cycles demands *stability of* Li metal anodes and high voltage cathodes. Such stability depends on the *interfacial structural evolution* during battery operation that is strongly affected by the nature and chemistry of the electrolyte. Optimizing the *structure, dynamics, and reactivity of electrolytes at interfaces* and their potential to induce *smooth Li deposition/stripping and nucleation/dissolution during longer times* is crucial to help stabilizing Li-metal anodes, with a subsequent huge impact on clean energy technologies.

Objective

Evaluate and characterize *interfacial phenomena* in Li metal anodes and develop strategies leading to *controlled reactivity* at electrode/electrolyte interfaces using advanced modeling techniques based on first-principles in close coordination with input from experimental collaborators. It addresses the understanding of life-limiting mechanisms taking into account microscopic phenomena.

Milestones

Time	Description (*status*)
June 2019	**Complete Stability Analysis of Current Best Electrolytes** (*Completed*)
September 2019	**Complete Elucidation of Roles of Salt Chemistry and Concentration** (*Completed*)
December 2019	**Complete Identification of Alternative Electrolytes** (*Completed*)
March 2020	**Complete Evaluation of Applied Potential on Reactivity** (*Completed*)
June 2020	Complete Evaluation of Partially Oxidized Li Substrates (*In progress*)
Go-No Go	Preliminary Electrolyte Design Validated to Achieve Performance Measures *(In progress, with PNNL collaborators*)
September 2020	Complete Elucidation of SEI Formation over Nucleating Li Structures (*In progress*)
December 2020	Complete Assessment of Electron and Ion Transfer during SEI Growth on Li Nuclei (*in preparation*)
March 2021	Final cell design and test

Approach

Methods

Structure and dynamics of existent best electrolytes and ion transport mechanisms under external electric fields characterized by ab initio and classical molecular dynamics.

Identification of new electrolytes is carried out correlating redox properties of complexes in solution with interfacial reactivity as evidenced by simulations and experiments.

Synergistic collaboration with PNNL (Zhang's group) for electrolyte test and design, and analysis of interfacial reactivity for Li anode and metal oxide cathodes.

Progress towards FY21 milestones

SEI chemistry and reactivity explained. Effect of applied external potential (quantum and classical physics approaches) on Li deposition identified. Current work includes studies of Li substrates containing natural impurities such as oxides or defective sites, and completing investigations (electron and ion transfer) during SEI nucleation/dissolution during Li deposition/stripping with selected best performance electrolytes. High voltage cathode interfacial phenomena will be also completed.

Technical Accomplishments: Stability Analysis of Best Current Electrolytes

DME ___ solvent

TFEO CF_3 ___ diluent

F_3C ___ O ___ O ___ CF_3

salt LiFSI
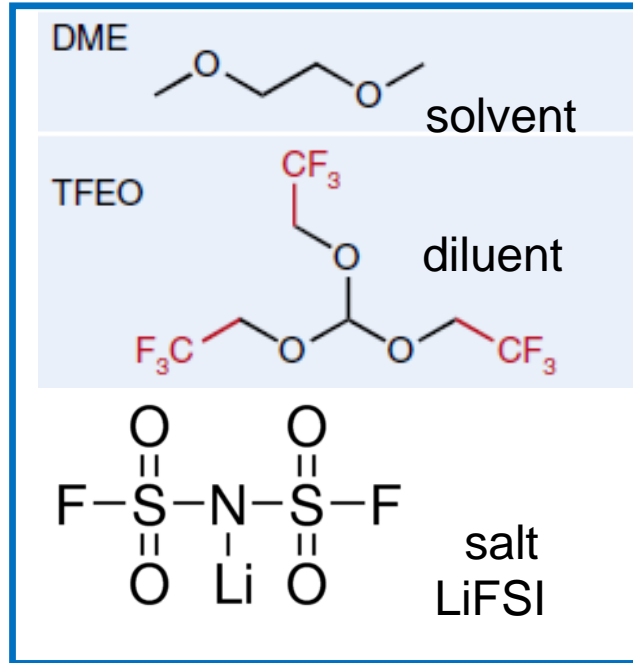
LiFSI: DME: TFEO
1:1.2:3 is a LHCE

We answer (next 7 slides)
why LHCEs perform
well at the Li anode surfaces,
elucidate structure and dynamics
and role of diluent

Localized high concentration electrolytes (LHCE) contain a salt dissolved in a mixture of solvent and diluent.
Our collaborators from PNNL have shown that LHCEs yield the current best battery performances at both Li anode and high voltage cathode interfaces
(Cao, Zhang, et al. Nature Energy, 2019, 796-805)
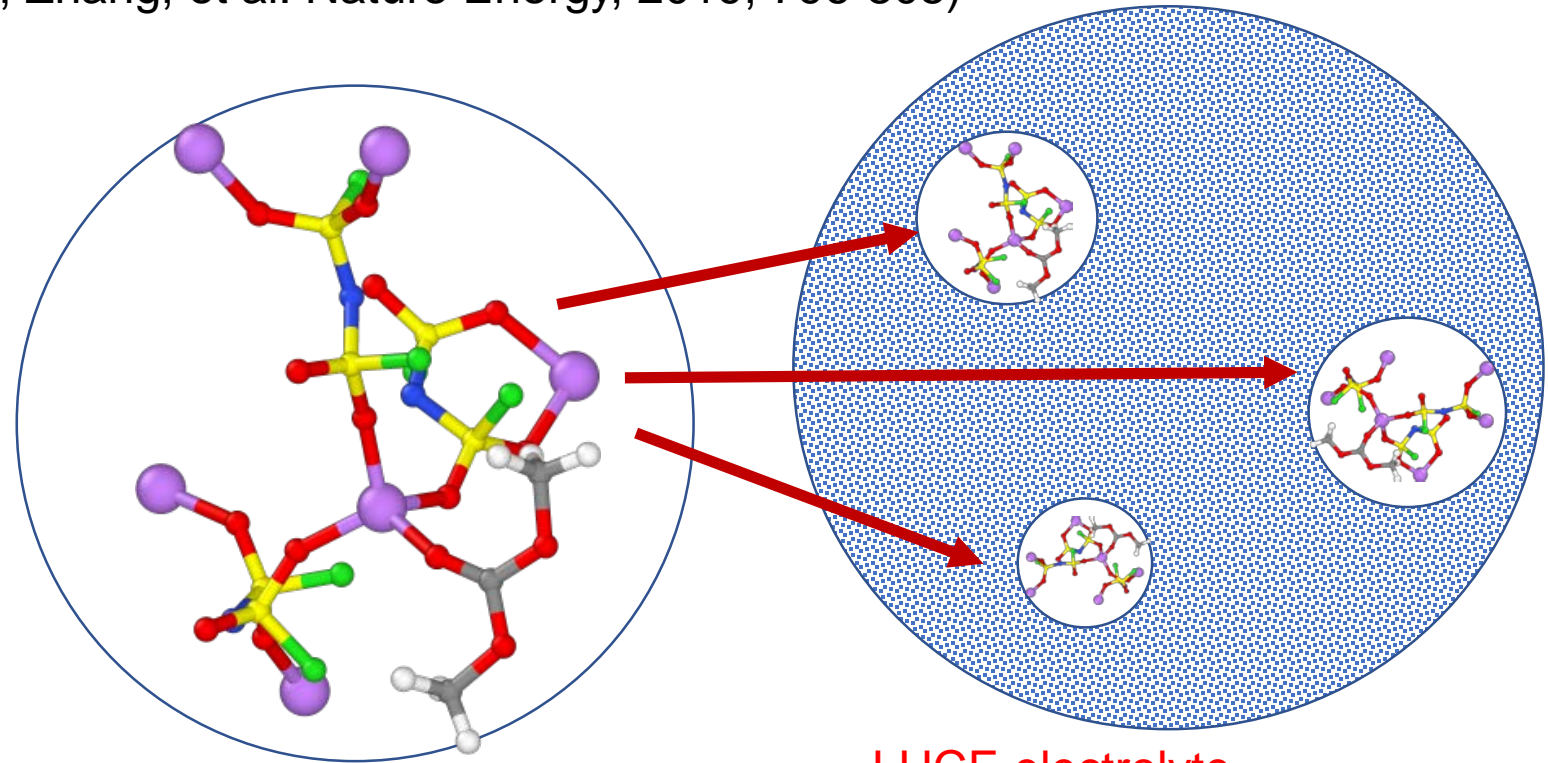
highly solvated Li ion structure typical of a high concentration electrolyte (HCE)

LHCE electrolyte
keeps HCE structure in localized pockets.
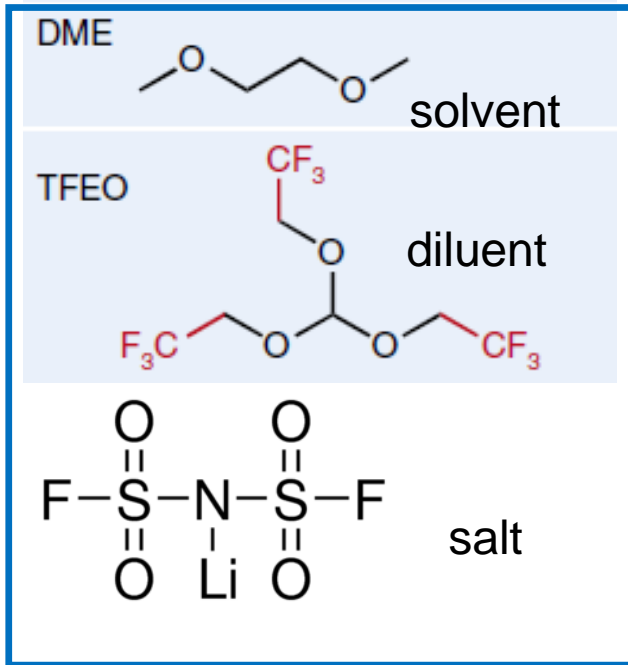Li-diluent interaction is weak; diluent reduces viscosity of solution

Technical Accomplishments: How do LHCE solutions help protecting the Li anode?

DME — solvent

TFEO — diluent

CF₃

F₃C ... O ... O ... CF₃

F–S–N–S–F (O, O, Li) — salt

LiFSI: DME: TFEO
1:1.2:3

Total decomposition of the anion leads to an atomically dispersed, thin SEI layer, that near the anode surface may be enriched by some LiF from the fluorinated diluent. Li ion diffusion through this thin layer should be uniform, causing uniform deposition underneath.

By choosing the correct diluent properties (reduction potential, oxidation potential, chemical structure) and concentration, LHCEs form a protective SEI
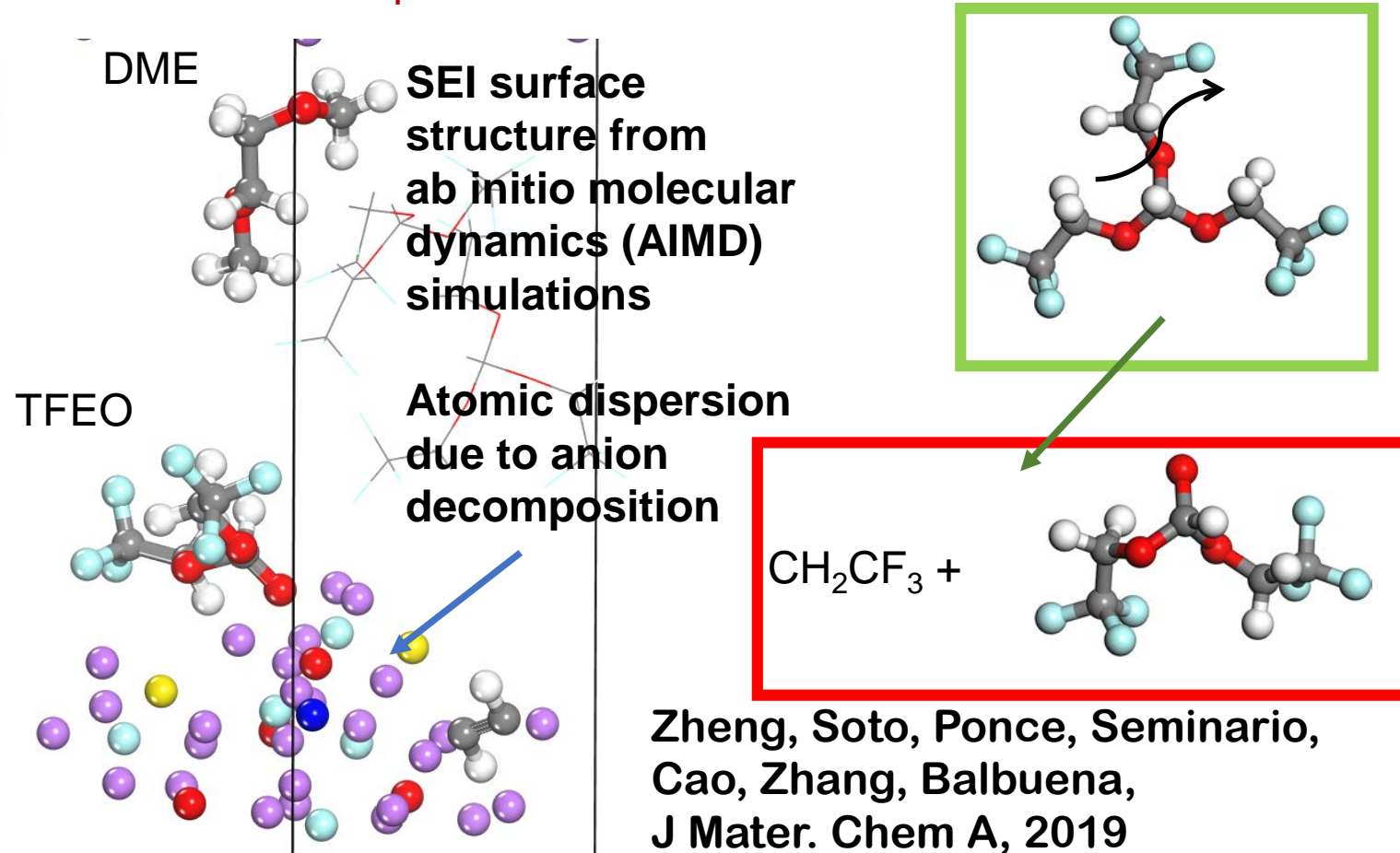**What is the structure of this protective SEI?**

LiFSI salt completely decomposes into atomic elements at the Li metal surface; TFEO diluent also decomposes near the surface

DME

SEI surface structure from ab initio molecular dynamics (AIMD) simulations

TFEO

Atomic dispersion due to anion decomposition

CH₂CF₃ +

Zheng, Soto, Ponce, Seminario, Cao, Zhang, Balbuena, J Mater. Chem A, 2019

Technical Accomplishments: Roles of Salt Chemistry and Concentration

Dilute electrolyte (1.2 M): isolated solvation complexes

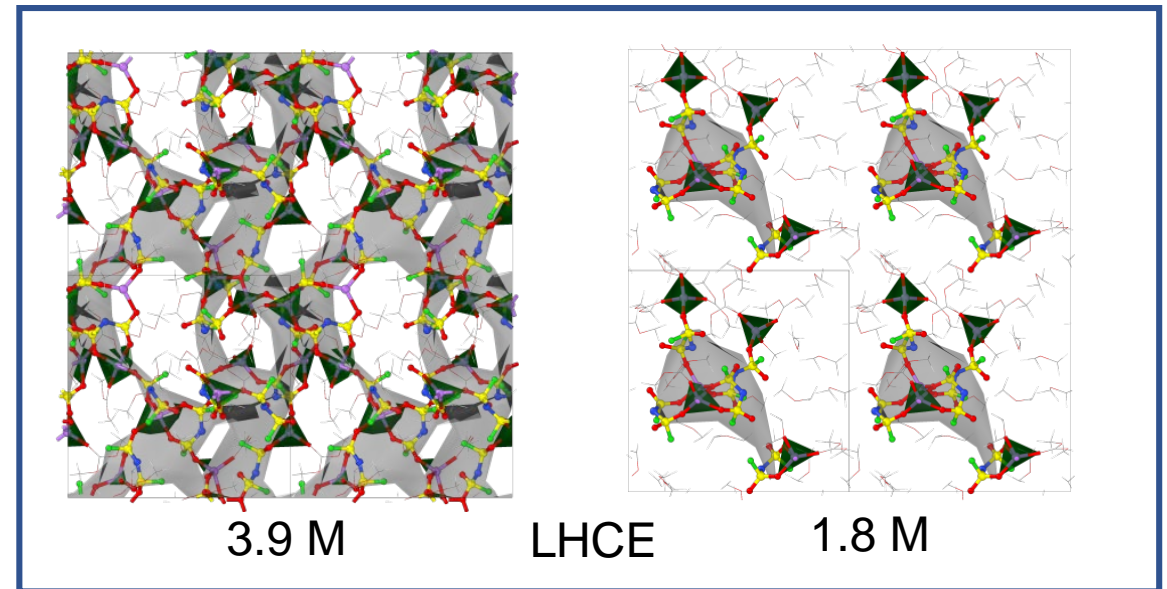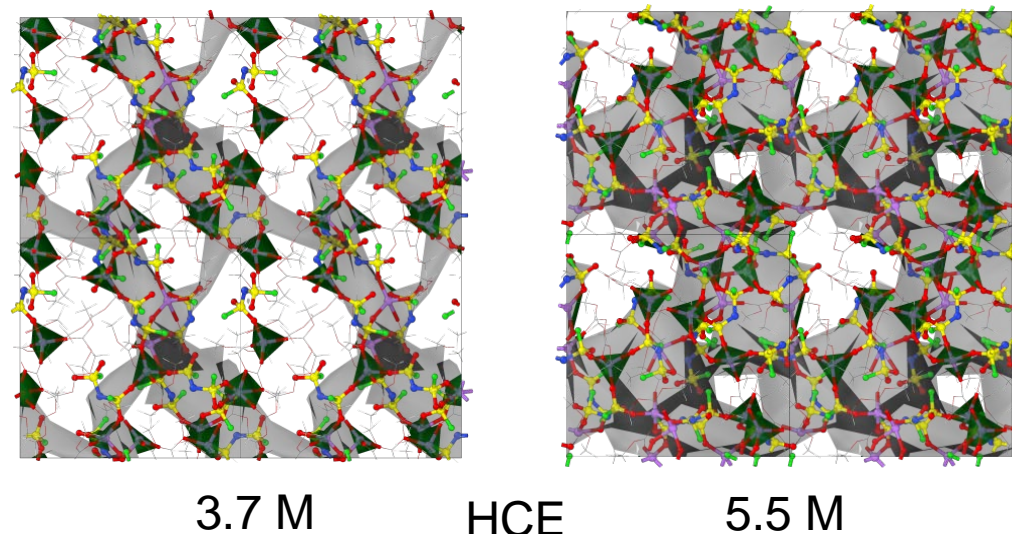Li is 4-coordinated with 3 DME and 1 FSI[-]
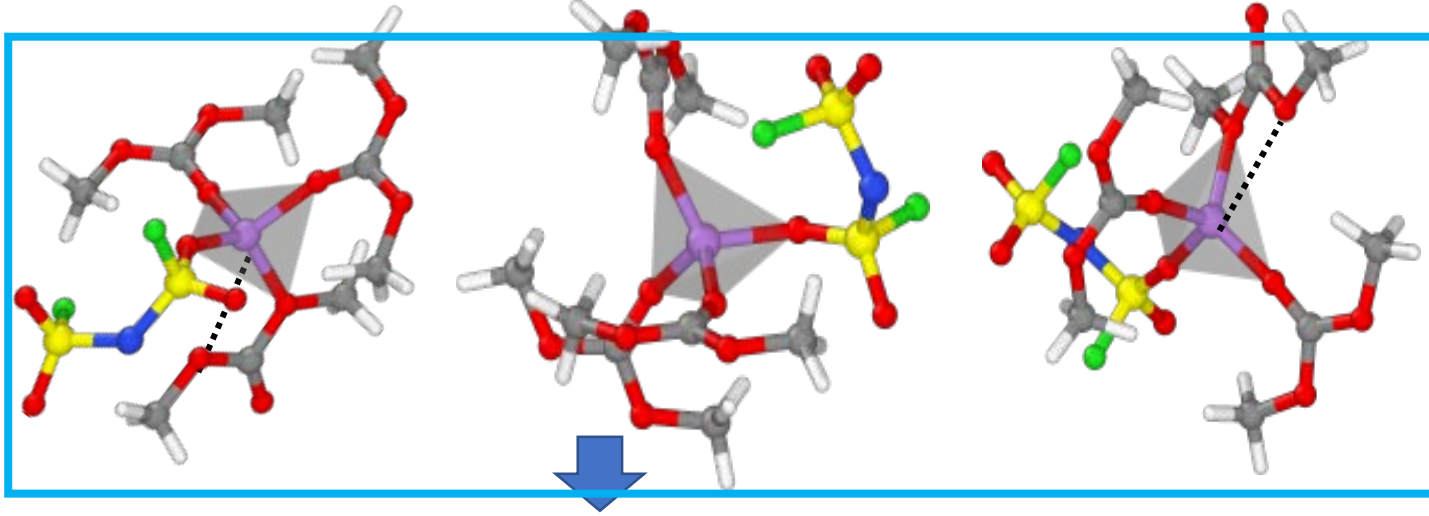
Here we show how tetrahedral solvation structure evolves as we change solvent chemistry and salt concentration
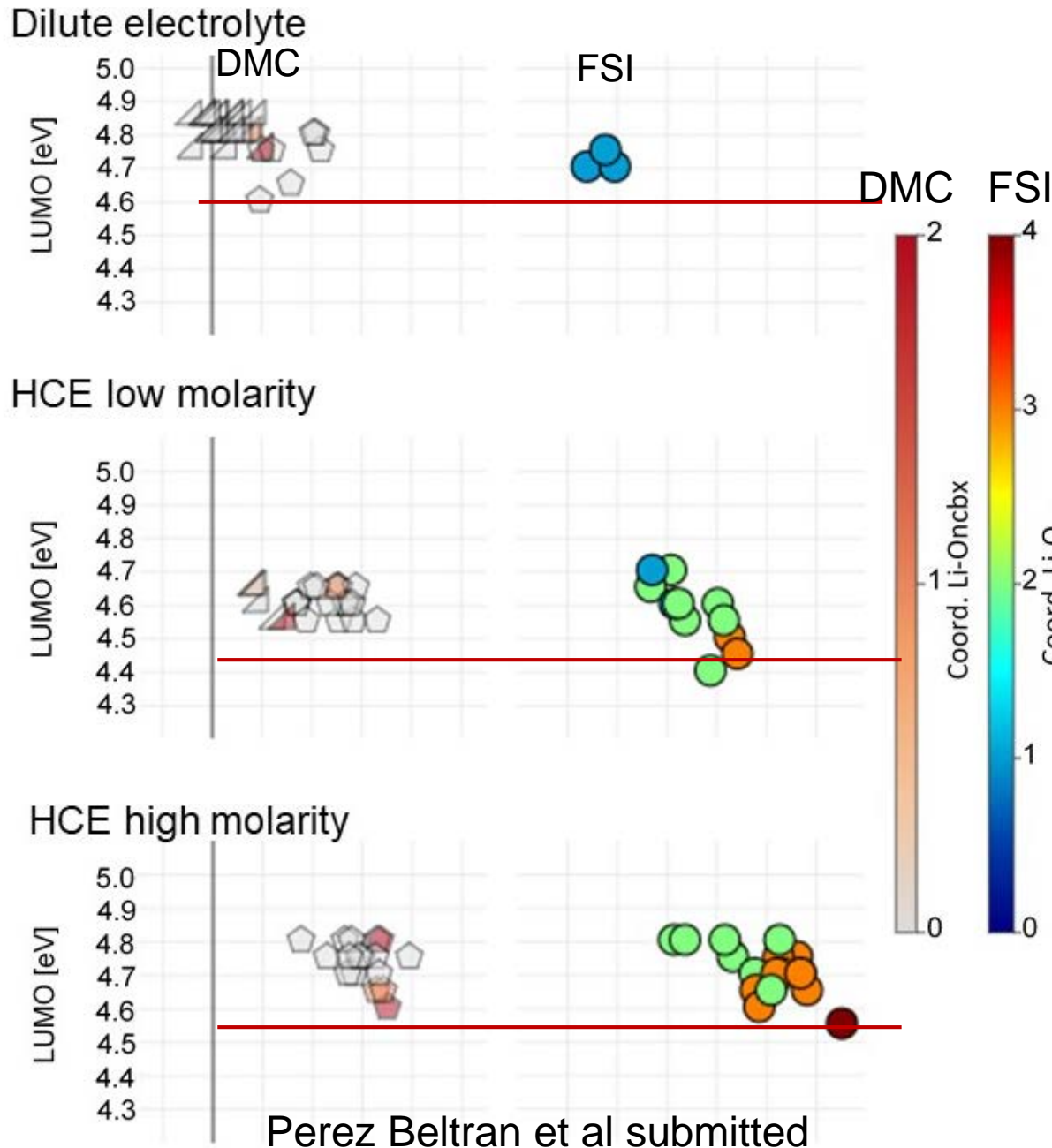
LHCE electrolytes: formation of pockets (grey regions structure previously speculated, **now confirmed by AIMD evidence**) separated by diluent islands (white regions)

What are the consequences on reactivity?

HCE electrolyte: 3D interconnected solvation networks

3.7 M   HCE   5.5 M

3.9 M   LHCE   1.8 M

SEI predictions from Computational Screening Method (**Dilute** and **HCE**)

Red line: energy level for reduction
Color bar: degree of coordination
Solvent molecules: two coordination modes (triangle & pentagon)

Dilute electrolyte: Low-coordinated DMC solvent molecules reduce first →Organic-based SEI

HCE 3.7 M: Anions of coordination 2-3 reduce first →Inorganic SEI

HCE 5.5 M: Coordination 3-4 anions reduce first. Highly coordinated DMC can contribute→ Inorganic (primary) & partially organic (secondary) SEI

Li-coordination and salt concentration: key for SEI chemistry

Perez Beltran et al submitted

Technical Accomplishments: Identification of Alternative Electrolytes
## SEI predictions from Computational Screening Method in LHCE electrolytes

LHCE electrolytes: DMC (solvent), BTFE (diluent), LiFSI (salt)
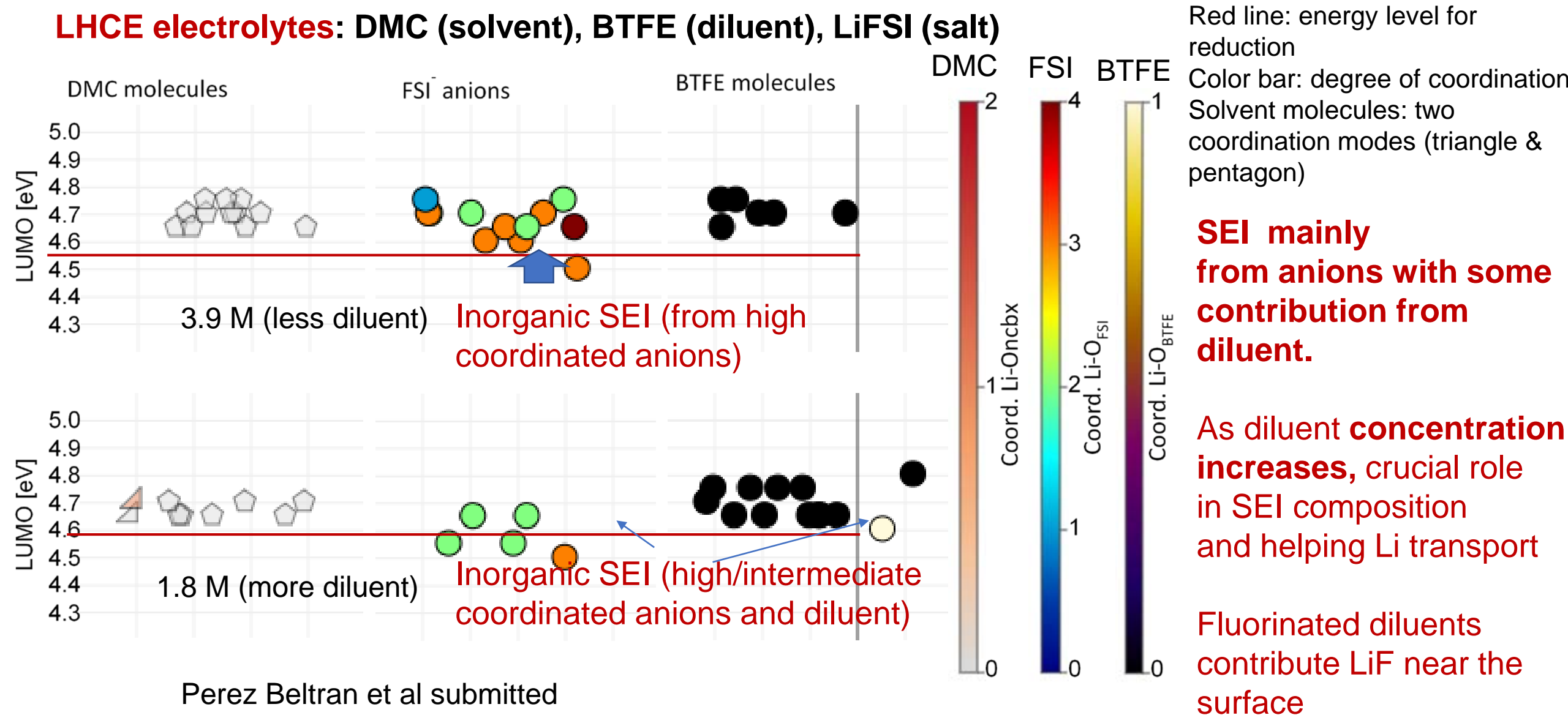
Red line: energy level for reduction
Color bar: degree of coordination
Solvent molecules: two coordination modes (triangle & pentagon)

DMC molecules
FSI⁻ anions
BTFE molecules
DMC   FSI   BTFE

LUMO [eV]

3.9 M (less diluent)

Inorganic SEI (from high coordinated anions)

1.8 M (more diluent)

Inorganic SEI (high/intermediate coordinated anions and diluent)

Perez Beltran et al submitted

Coord. Li-Oncbx
Coord. Li-O_FSI
Coord. Li-O_BTFE

SEI mainly from anions with some contribution from diluent.

As diluent **concentration increases,** crucial role in SEI composition and helping Li transport

Fluorinated diluents contribute LiF near the surface

Technical Accomplishments: Identification of Alternative Electrolytes
CEI predictions from Computational Screening Method (Dilute and HCE)

Perez Beltran et al, submitted

Analysis of oxidation reactions: cathode side
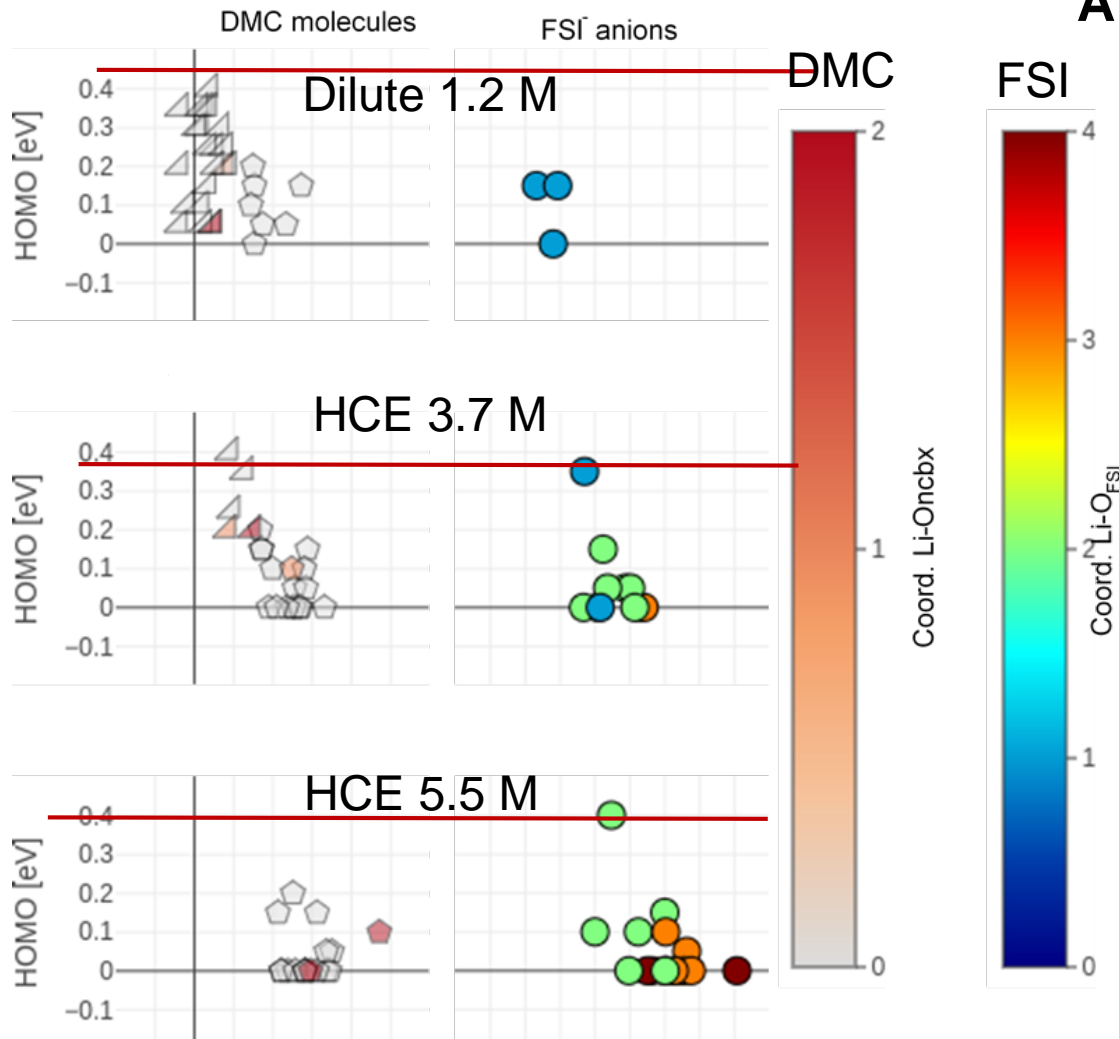
red line → suggests oxidation reaction;
Color bar: degree of coordination
Solvent molecules: two coordination modes (triangle & pentagon)

In **dilute electrolytes**, low coordinated solvent molecules (like DMC) are the easiest to oxidize → **Organic CEI**

Intermediate molarity HCE: low-coordinated anions become as oxidizable as solvent;

High molarity HCE: anions of intermediate coordination are the most oxidizable
→ **Mixture of Inorganic and organic CEI expected (more inorganic as molarity increases)**

Important: CEI based on organic molecules will be highly porous and less useful to control metal oxide phase transformations, metal dissolution, and cathode structure collapse.

Technical Accomplishments: Identification of Alternative Electrolytes
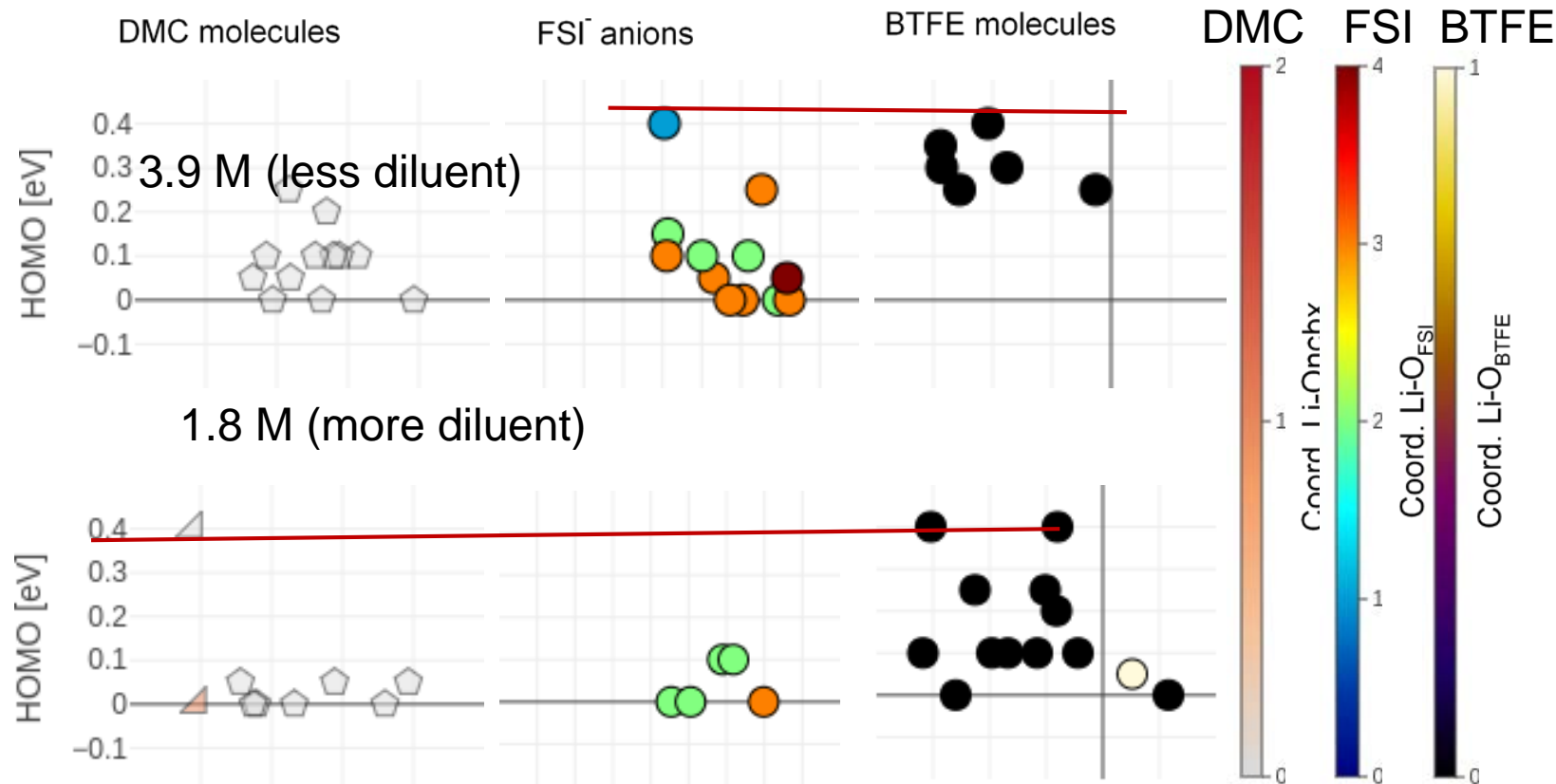## CEI predictions from Computational Screening Method (LHCE)

Analysis of oxidation reactions: cathode side

red line → suggests oxidation reaction;
Color bar: degree of coordination
Solvent molecules: two coordination modes
(triangle & pentagon)

LHCE electrolytes

With relative low amounts of diluent, intermediate coordinated anions and diluent molecules contribute to CEI
→ **Inorganic CEI**

With higher amount of diluent, higher HOMO levels are dominated by low coordinated diluent molecules.
→ **Inorganic CEI: composition can be tuned with chemistry of diluent.**

Useful to control metal oxide phase transformations, metal dissolution, and cathode structure collapse.

Technical Accomplishments: Evaluation of Applied Potential on Reactivity

Impact on ion transport mechanisms in LHCE electrolytes
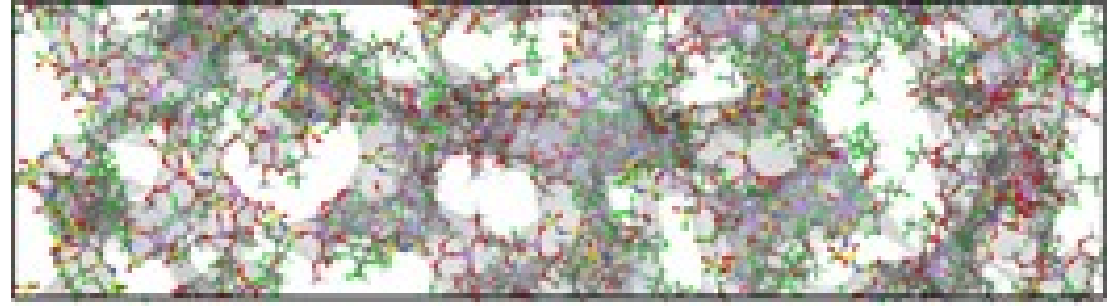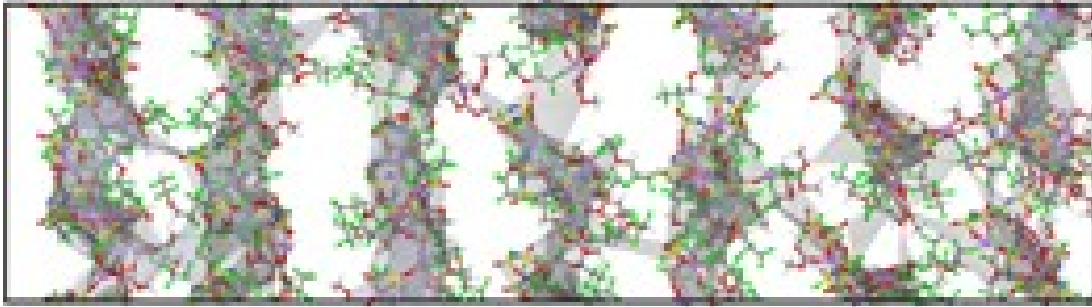
Left: Structure of LHCE electrolyte showing extended 3D network, before applying electric field. Grey regions are Li-solvated structures usually including salt (LiFSI), and sometimes solvent (DME) or diluent (TTE). White regions contain solvent and diluent molecules (not shown) that do not solvate ions. Right: Same 3D network after 0.4 nanoseconds under an electric field. Structure is preserved.


Li^+

Li^+

Ion trajectories (**dark lines**) under an external electric field. The simulation cell has a source of Li ions at the left of the cell and a sink of Li ions at the right. Ions move from pocket to pocket with the help of the diluent.

Perez Beltran and Balbuena, work in progress

Technical Accomplishments: Ion Diffusion in Solid State Electrolytes
Li-metal/Li$_9$N$_2$Cl$_3$ interfaces

Interface I Interface II
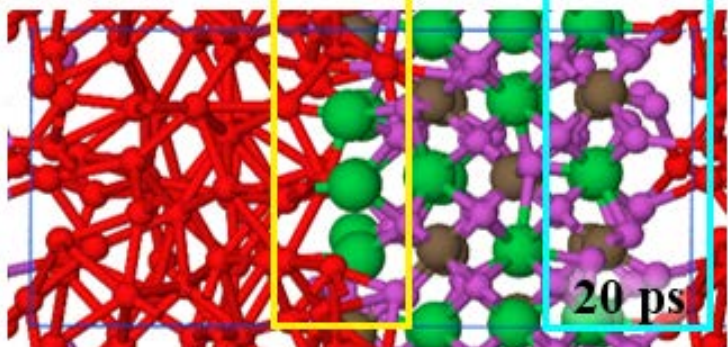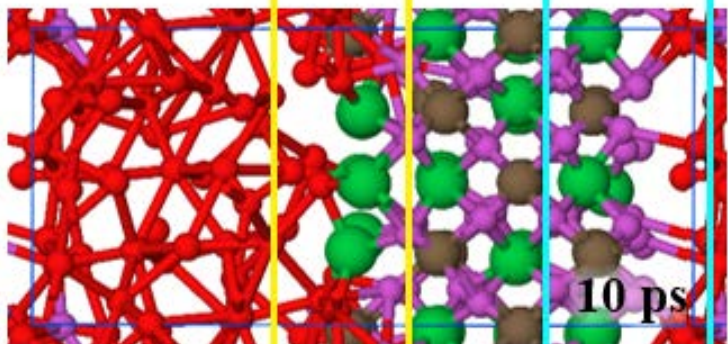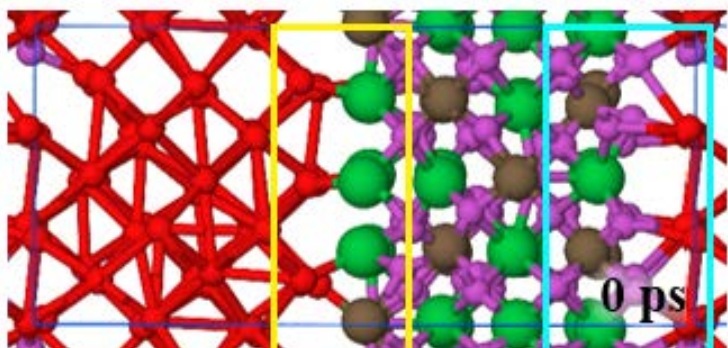
Li-ion (purple), Li-metal (red), Cl (green), N (brown)

(right) Li-ion diffusion pathways (purple) through vacancies in Li$_9$N$_2$Cl$_3$ solid electrolyte

Li-ions circumvent anions during their diffusion

Anions remain almost immobile facilitating Li-cation transport

Li-metal   Li$_9$N$_2$Cl$_3$ Li-metal

# of Li coordinated with Cl

# of Li coordinated with N

2.6 Å

Li-metal   Li$_9$N$_2$Cl$_3$

Galvez and Seminario, JES 2019
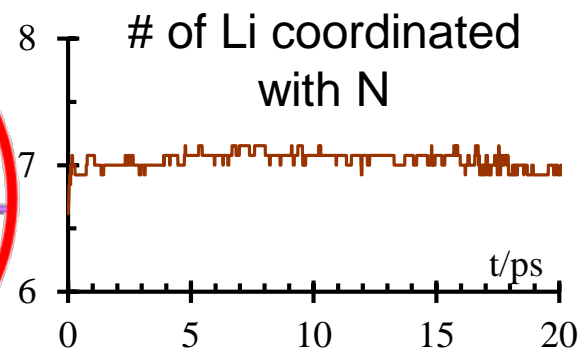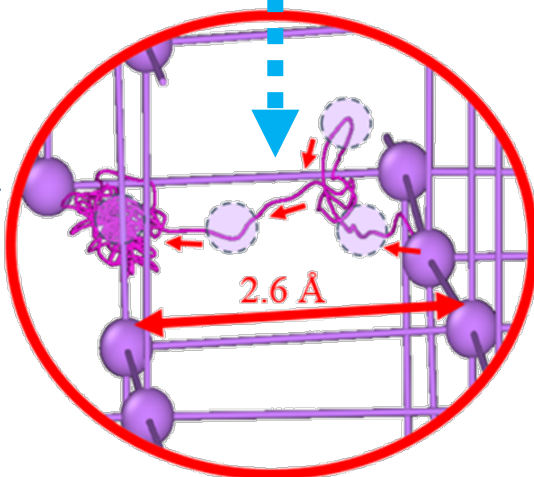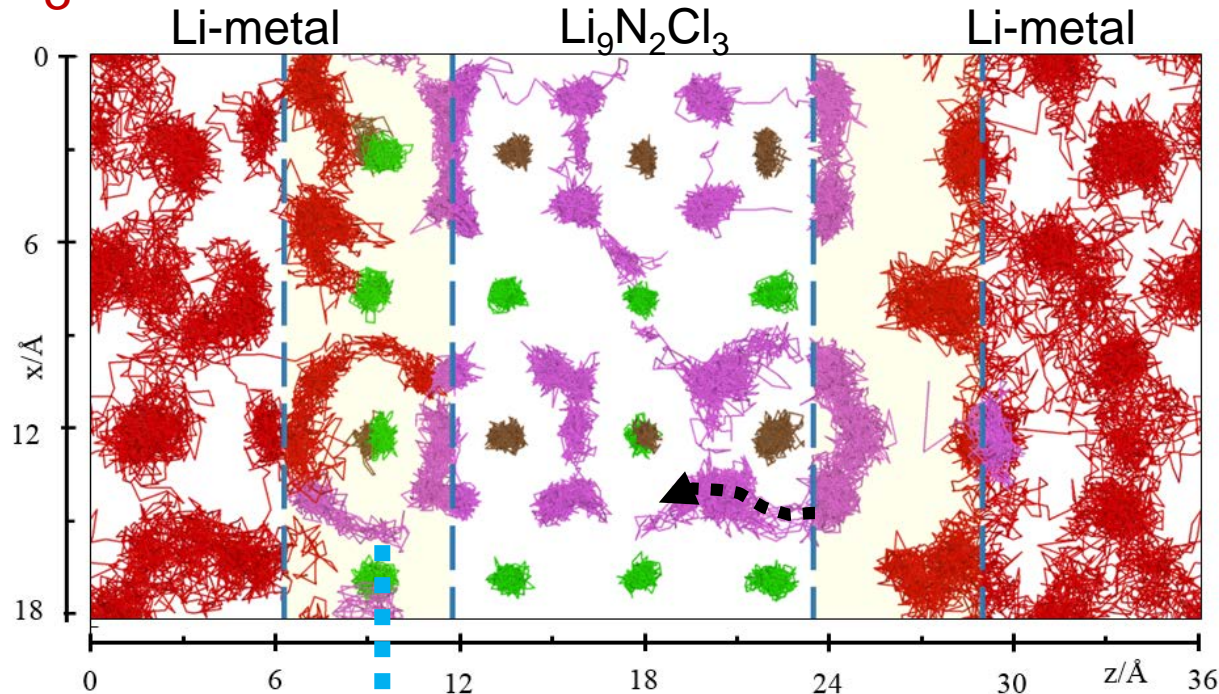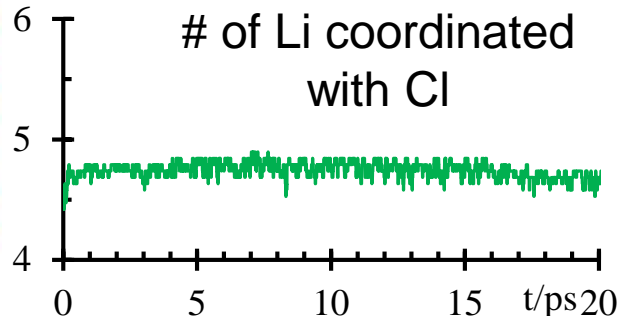
Technical Accomplishments: Evaluation of an Applied Potential on Reactivity

Potential energy profile per Li-ion (E_{Li}) through the nanobattery simulation cell in the absence of an external electric field

Li-ions from the anode spontaneously fall to the cathode during discharge, where they are more stable, corresponding to an output voltage of 3.86 volts.

Li metal anode covered by Li_3P & Li_2S (SEI products of decomposition of solid electrolyte $Li_7P_2S_8I$); $LiCoO_2$ as cathode material.
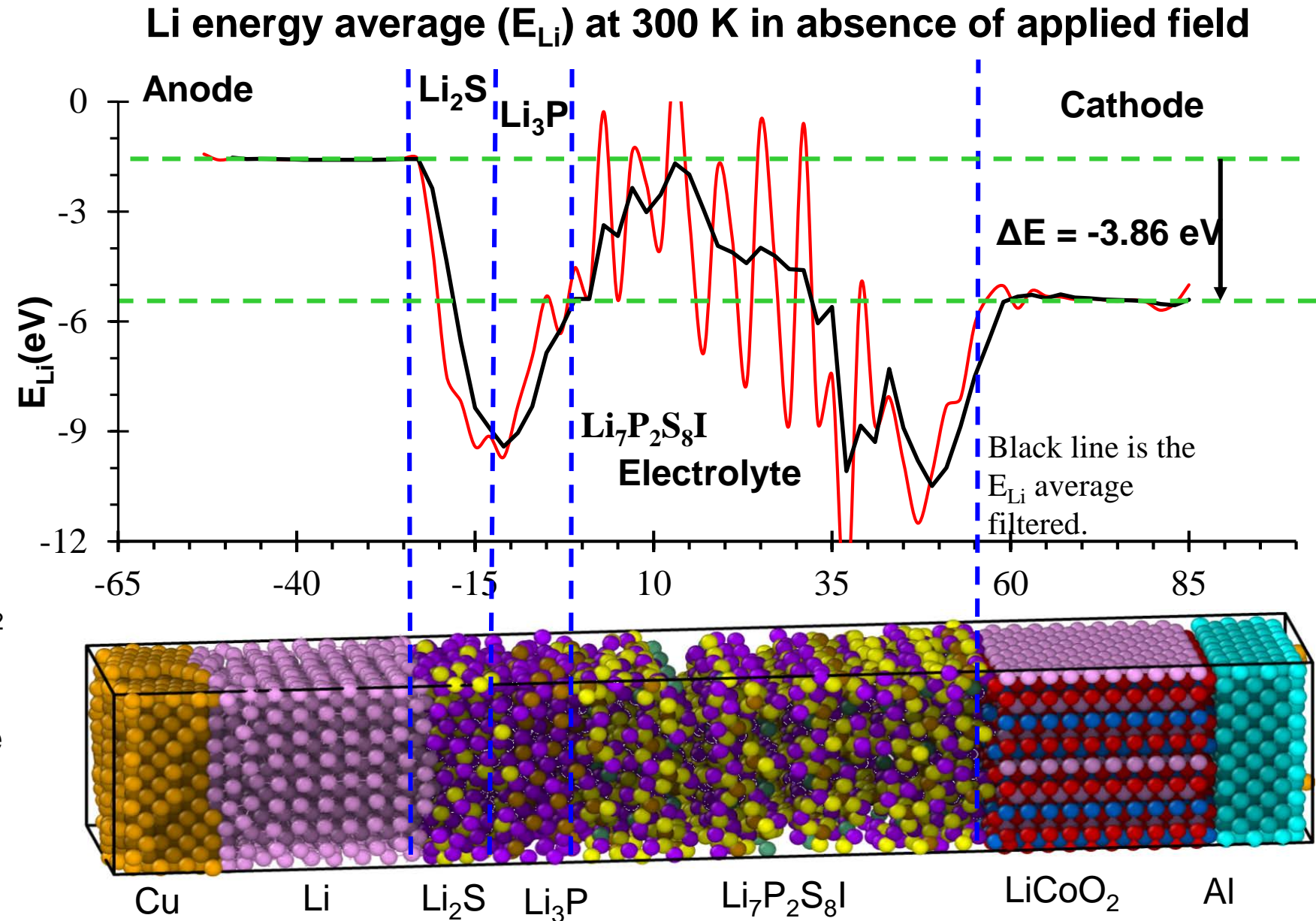
Energy drops as Li goes through the SEI (coulombic interactions), and increases at both double layers. It remains constant at both electrodes.

Li energy average (E_{Li}) at 300 K in absence of applied field

Anode — Li_2S — Li_3P — Cathode

$\Delta E = -3.86$ eV

$Li_7P_2S_8I$ Electrolyte

Black line is the E_{Li} average filtered.

E_{Li}(eV)

Cu Li Li_2S Li_3P $Li_7P_2S_8I$ $LiCoO_2$ Al

Ponce and Seminario, manuscript in preparation

Li energy average (E_{Li}) at 300 K in presence of $E_F = 0.75$ V/Å
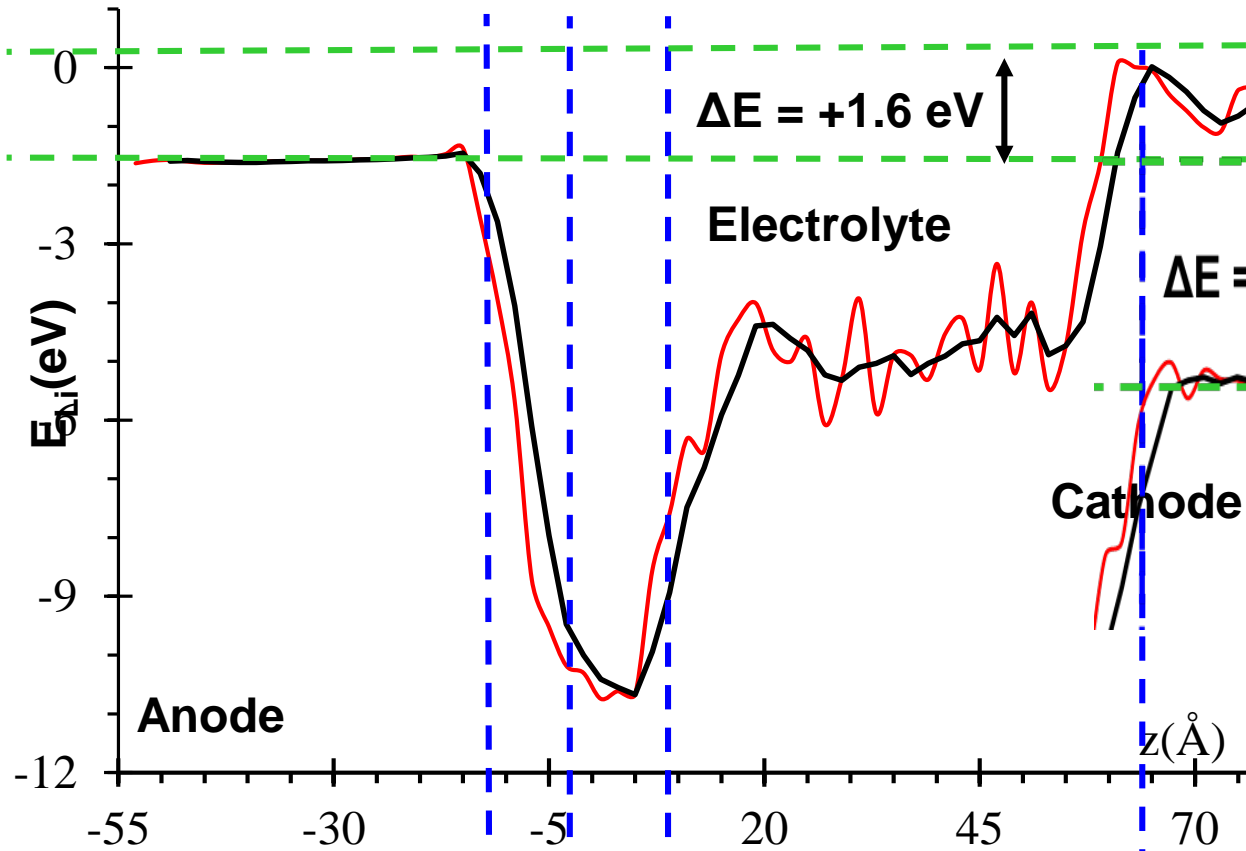
Potential energy profile per Li-ion (E_{Li}) through the nanobattery simulation cell in presence of an external electric field of E_F = 0.75 V/Å (actual data, red; filtered data, black)

Li-metal anode is covered by Li_3P/Li_2S SEI decomposition products of solid electrolyte $Li_7P_2S_8I$; $LiCoO_2$ is the cathode material.

The externally applied electric field now have to neutralize the open-circuit voltage of 3.86 V and adds an additional 1.6 V in this case, to allow Li-ions to move up to the anode during charge of the nanobattery. This is equivalent to a charging voltage of 5.46 V.

Ponce and Seminario, manuscript in preparation
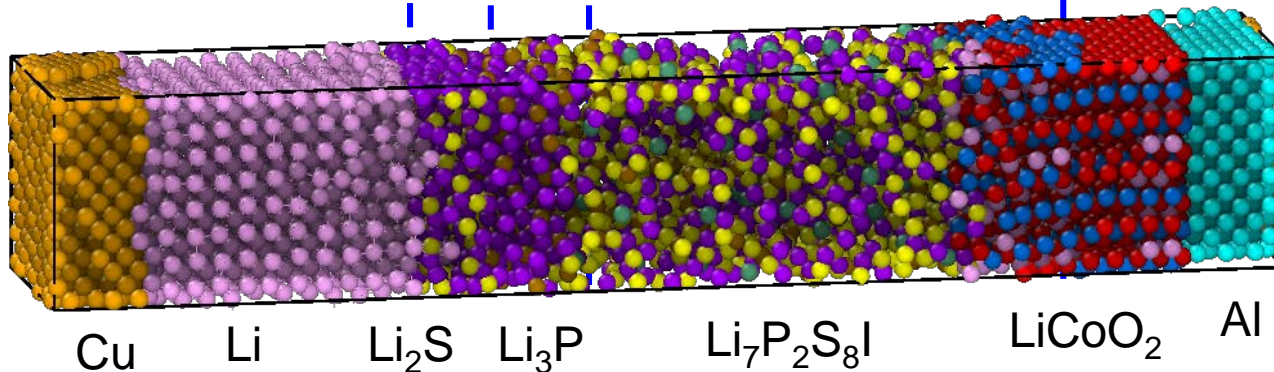
Technical Accomplishments: Evaluation of Applied Potential on Reactivity

AIMD simulation cell contains a Li surface (uncharged or charged) in contact with electrolyte

a) 2M LiTFSI

uncharged Li surface
DME not reduced

c) 2M LiTFSI

charged Li
surface
DME reduction
depends on salt type
and concentration

b) 2M LiTFSI

2M LiFSI
Li oxidation

d) 2M LiTFSI

less Li
oxidation

2M LiFSI

	1M (C1)	1M (C2)	2M		1M (C1)	1M (C2)	2M		DME	DME:DOL	DOL	
	🟦	🔺	⬭ LiTFSI		🟥	🔺	⬭ LiFSI		🔶	🔷	🔷	No Salt
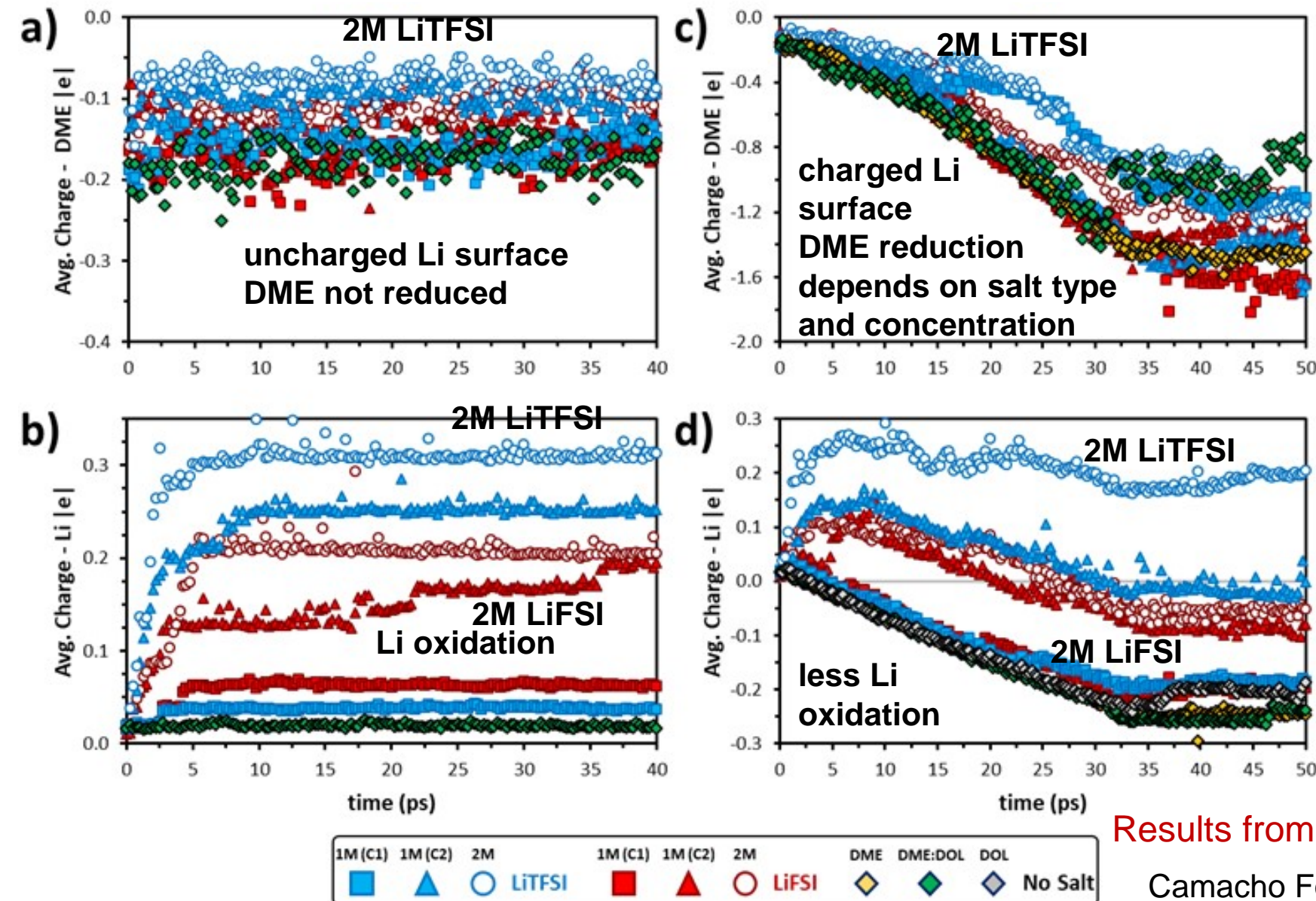
DME solvent reduction in 1M and 2M electrolyte solutions of LiFSI or LiTFSI (symbols in bar at the bottom)
a) On uncharged Li surfaces, average charge is ~ -0.15; DME is not reduced.
c) On charged Li surfaces, DME is reduced faster in 1M than in 2M LiFSI solutions. Reduction is slower in LiTFSI solutions (2M is the slowest).

Li metal oxidation: b) On uncharged Li surfaces, Li becomes oxidized in contact with the electrolyte solution. The degree of oxidation depends on the electrolyte (higher for 2M than 1M, and higher in LiTFSI than in LiFSI solutions.
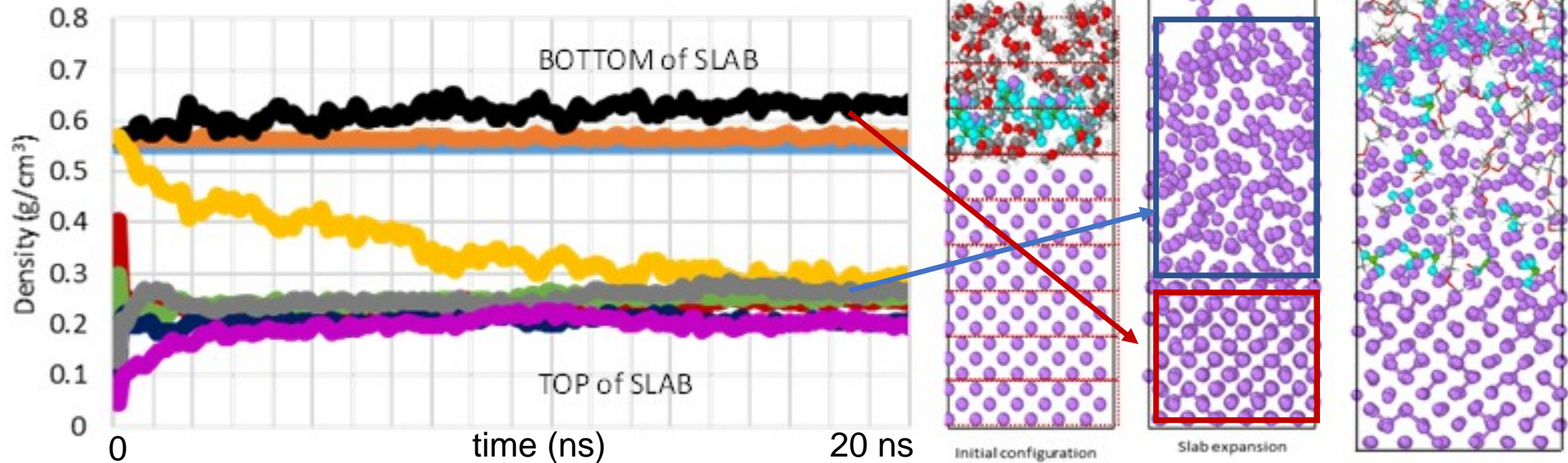**d) On charged Li surfaces**, some electrolytes (eg. 2M LiTFSI) oxidize the surface, others much less.

Results from ab initio MD under applied fields

Camacho Forero and Balbuena, submitted

Work in progress: SEI nucleation and growth studies

Density changes in Li slab: bottom layers keep Li metal density

Top of Li slab layers dissolve due to Li oxidation and SEI formation

Classical MD simulations using reactive force fields allow us to detect: a) Expansion and density changes in the Li phase, b) following nucleation of components (for example LiF) as a function of Li thickness, electrolyte composition, salt concentration.
Future work will include Li nucleation after initial SEI is formed and simultaneous observation of Li nucleation and SEI growth

Any proposed future work is subject to change based on funding levels

Work in progress: Artificial intelligence for MD simulations

② CMD Simulations

FF data

atom types

Parameters per CMD simulation:
Thickness$_{SEI}$: $\delta_{(\varepsilon,t,l)}$ / $\delta_{(I,t,l)}$ / $\delta_{(T,t,l)}$
Mobility: $\mu_{(\varepsilon,t,l)}$ / $\mu_{(T,t,l)}$ / $\mu_{(CC,t,l)}$
Diffusion: $D_{(\varepsilon,t,l)}$ / $D_{(T,t,l)}$ / $D_{(CC,t,l)}$
Young Mod: $Y_{(\varepsilon,t,l)}$ / $Y_{(T,t,l)}$ / $Y_{(I,t,l)}$
Conductivity: $\sigma_{(\varepsilon,t,l)}$ / $\sigma_{(T,t,l)}$ / $\sigma_{(I,t,l)}$
Other: SSE thickness, SSE porosity,,
Crystallographic structure, Volume
expan. AIMD: DOS, Charge, density

ML: classifiers

ML: clustering

Atomic environments

ML: neural network

ns / nm

Resolution

Timescale / System size

ps / Å

atomic parameters

NNs
$b_1, b_2, \ldots, b_n$
$k_1, k_2, \ldots, k_n$
q_i
$\theta_1, \theta_2, \ldots, \theta_m$
m

k_1
q
b_1
m
θ_1
b_n
k_n
r

e.g., thickness $\delta_{(\varepsilon,t,l)}$

ε
t
l

hidden layers

δ

mono-physics model
$\delta_{(\varepsilon,t,l)}$

multi-physics model
$\delta(\varepsilon, T, CC, t, l)$

ε
t
l
I/V
T

Hidden layers

δ
D
Y
σ

① QMD Simulations

Ab-Initio Cell

h / mm

③ Neural network extrapolation

A
δ
SEI
SSE
K

Responses to Previous Year Reviewers' Comments

Project was not reviewed last year

Collaboration and Coordination with Other Institutions

- We collaborate closely with the group of Dr. Ji-Guang (Jason) Zhang at PNNL that develops the localized high concentration electrolytes (LHCEs). They have provided us with several formulations and their corresponding battery tests. We have developed a computational screening method to determine the electrolyte structure and ion transport mechanisms, as well as the optimum formulation and the predicted composition of SEI and CEI layers. This interaction has been really successful.

- In addition, we have recently started a new collaboration with Dr. Jun Liu and Dr. Jie Xiao from PNNL related to predictions of SEI nucleation on Li metal of variable thicknesses.

Remaining Challenges and Barriers

Predicting lifetimes in battery systems is a great challenge especially because of its non-equilibrium and extraordinarily complex nature. However, capacity loss and materials degradation are two of the main contributors to determining battery lifetimes. We expect that our new computational screening and predictive methodologies (in some cases aided by artificial intelligence methods) and a coordinated theoretical-experimental effort can move our work in the direction of achieving this crucial goal.

Proposed future work

Future work includes:

- Studies of Li substrates containing natural impurities such as oxides or defective sites
- Completing investigations (electron and ion transfer) of SEI nucleation/dissolution during Li deposition/stripping with selected best performance electrolytes
- Investigate effect of Li metal thickness on battery performance (collaboration with Jun Liu and Jie Xiao (PNNL)
- High voltage cathode interfacial phenomena (collaboration with Jason Zhang and Xia Cao, PNNL)
- Development of new force fields for improved classical MD simulations using artificial intelligence techniques

Any proposed future work is subject to change based on funding levels

Summary Slide

- **Accomplishments:**
  - We have elucidated the structure and ion transport mechanisms of the current best electrolytes for Li metal anodes and high voltage cathodes. We developed a computational screening method that allows prediction of components of interfacial layers at anode (SEI) and cathode (CEI) respectively. This method allows us to identify the optimum electrolytes for best battery performance.
  - We have investigated the effect of applied fields on the reactivity and ion transport in electrolyte solutions and at interfaces.

- **Technical highlights:**
  - We showed that tuning the diluent chemistry and composition, mostly inorganic cathode interfacial layers can be induced. This property is expected to provide stability to high voltage cathodes during delithiation.

- **Impact to VTO objectives:**
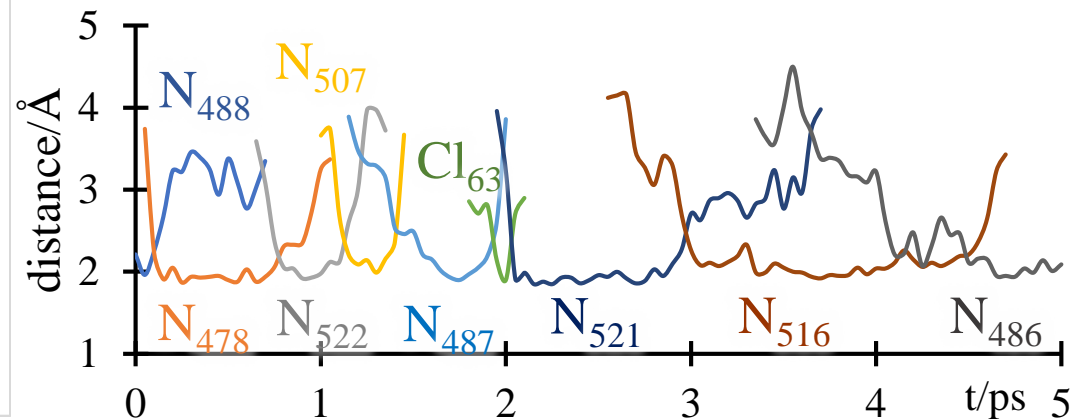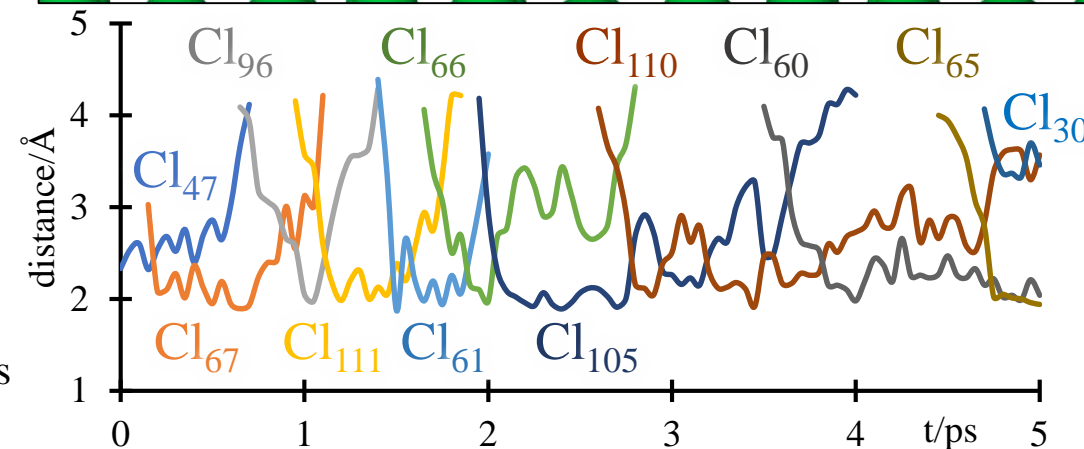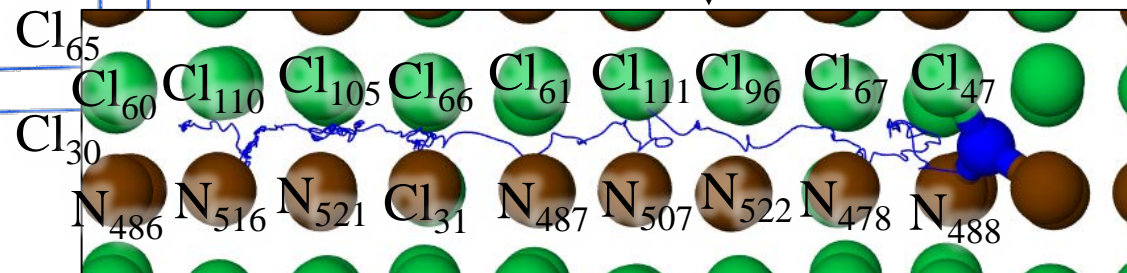 - The new insights developed in our work are directly related to the goals set in the Battery 500 program.

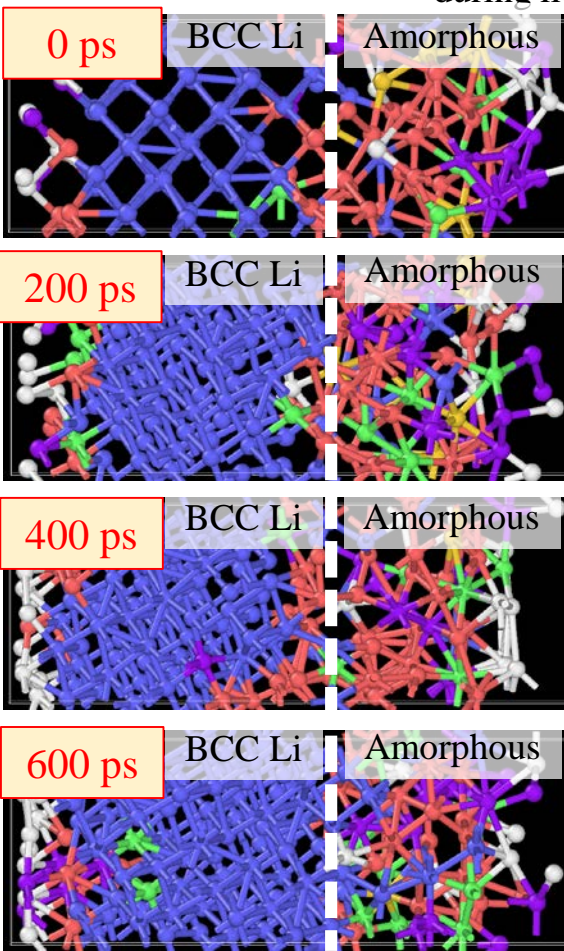# Technical Back Up Slides (maximum 5)

Nano-battery model: Li-metal/Li$_9$N$_2$Cl$_3$/NMC
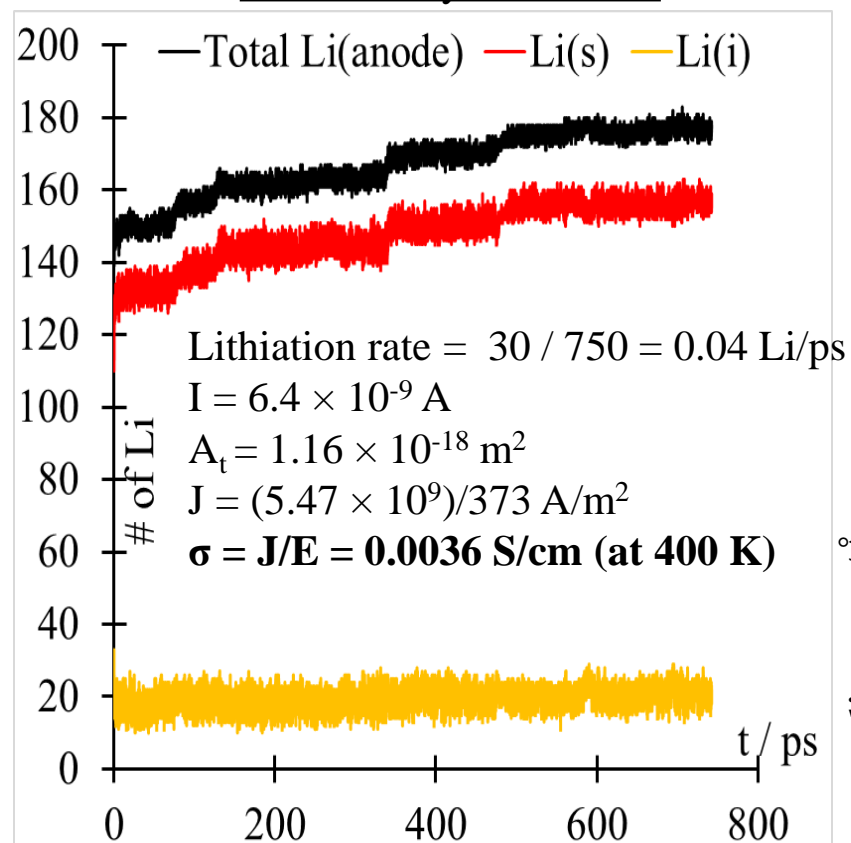
N   Li   Cl   Li$_m$ Li$_{(i)}$

Trajectory of a Li-ion through the electrolyte (5 ps)

$\mathcal{E}$ = 0.75 V/Å

A two phase mechanism is observed
during lithiation of the metal anode

Cl$_{65}$

Cl$_{60}$ Cl$_{110}$ Cl$_{105}$ Cl$_{66}$ Cl$_{61}$ Cl$_{111}$ Cl$_{96}$ Cl$_{67}$ Cl$_{47}$

Cl$_{30}$

N$_{486}$ N$_{516}$ N$_{521}$ Cl$_{31}$ N$_{487}$ N$_{507}$ N$_{522}$ N$_{478}$ N$_{488}$

0 ps	BCC Li	Amorphous
200 ps	BCC Li	Amorphous
400 ps	BCC Li	Amorphous
600 ps	BCC Li	Amorphous

Conductivity calculation

—Total Li(anode) —Li(s) —Li(i)

Lithiation rate = 30 / 750 = 0.04 Li/ps
I = 6.4 × 10^{-9} A
A$_t$ = 1.16 × 10^{-18} m^2
J = (5.47 × 10^9)/373 A/m^2
σ = J/E = 0.0036 S/cm (at 400 K)

# of Li

t / ps

Cl$_{96}$ Cl$_{66}$ Cl$_{110}$ Cl$_{60}$ Cl$_{65}$

Cl$_{47}$

Cl$_{30}$

Cl$_{67}$ Cl$_{111}$ Cl$_{61}$ Cl$_{105}$

distance/Å

t/ps

N$_{488}$ N$_{507}$

Cl$_{63}$

N$_{478}$ N$_{522}$ N$_{487}$ N$_{521}$ N$_{516}$ N$_{486}$

distance/Å

t/ps

MD with EF = 0.75V/Å of $Li_{1680}P_{480}S_{1920}I_{240}$ $(Li_7\text{-}PS_4\text{-}PS_3I\text{-}S)_{240}$ SSE battery

Angle distribution S-Li-S

Angle distribution Li-S-Li

Angle distribution S-P-S

S-P-S of PS_4 with EF ~110 °, initial structure (110°)
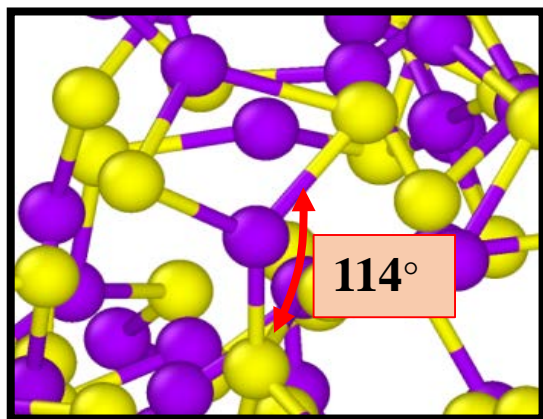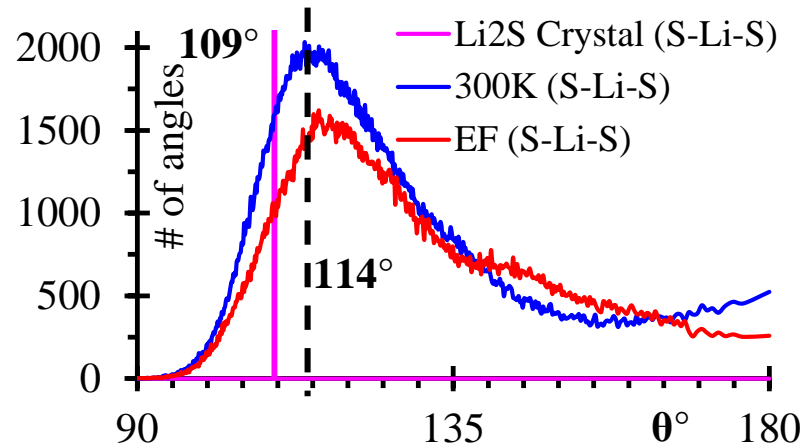
S-Li-S with EF ~114 °, Li_2S crystal pure (109°)
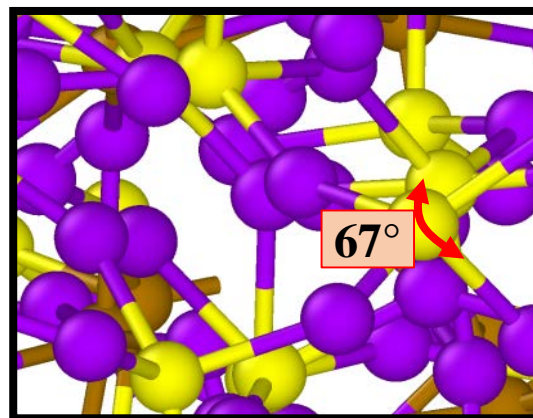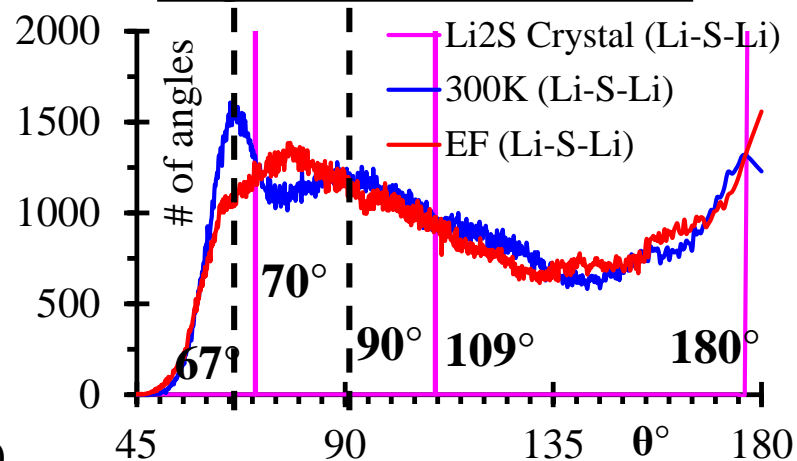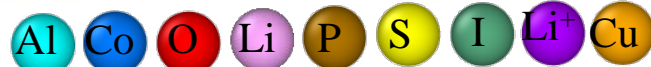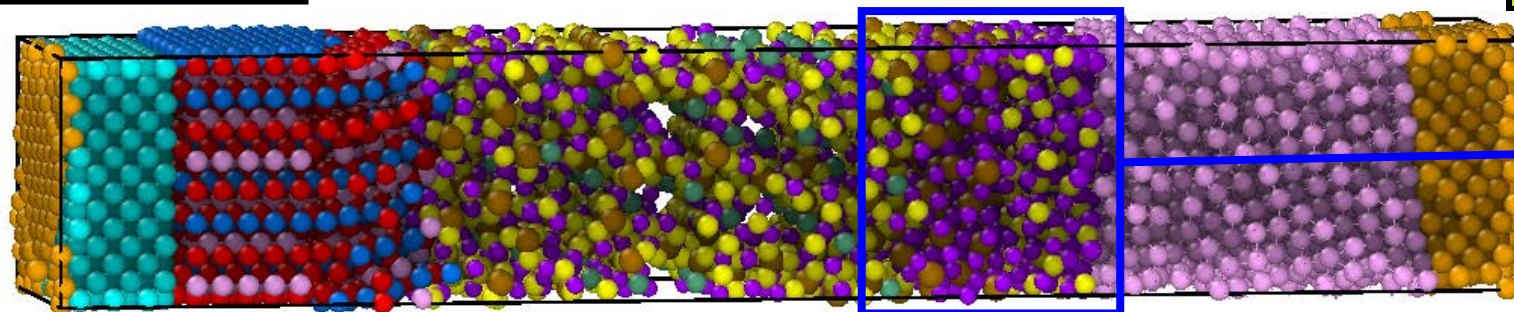
Li-S-Li with EF ~67 °, Li_2S crystal pure(70°)
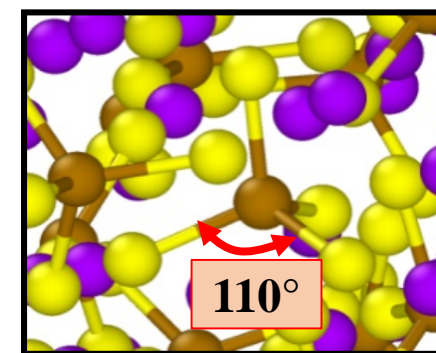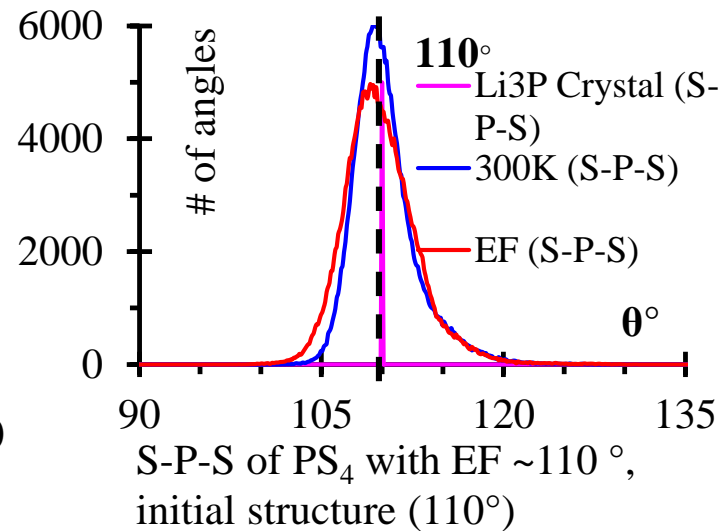
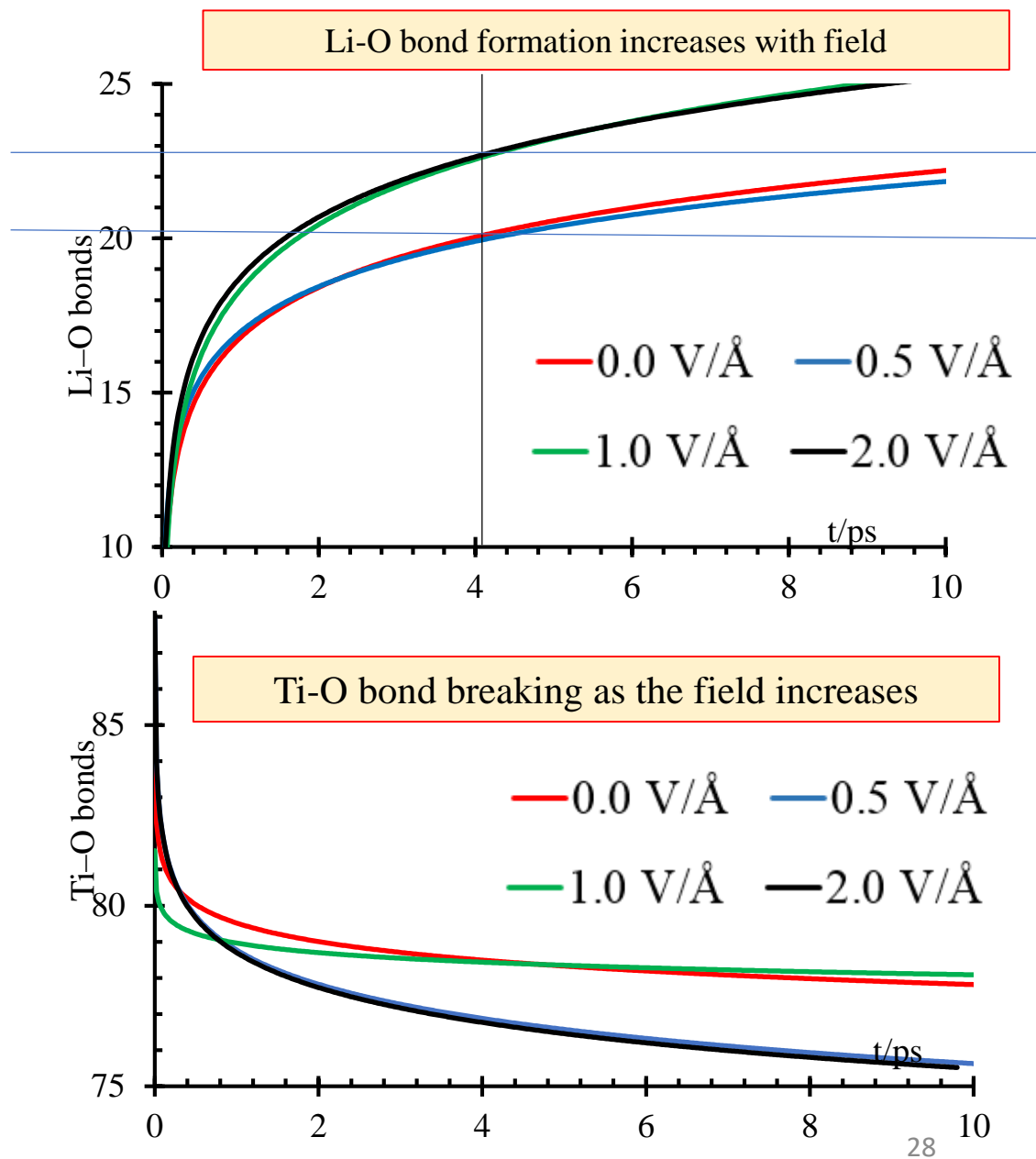PS_4 dissociates in a few amount during MD and maintains their original shape (tetrahedral)

SEI:
Li_2S
Li_3P

EF = 0.75 V/Å

Al Co O Li P S I Li⁺ Cu

La$_{2/3-x}$Li$_x$TiO$_3$/Li-metal(001) interface, external electric field $\mathscr{E}$: bonds formation/breaking

SQE: AIMD DFT PBE, τ = 0.5 fs, t_{MD} = 20 ps, E_{cutoff} = 40 Ry (λ_{cutoff} = 0.5 Å)

10 ps

Electric field favors the formation of Li$_2$O

$\mathscr{E}$ = 0 V/Å

$\mathscr{E}$ = 0.5 V/Å

$\mathscr{E}$ = 1 V/Å

$\mathscr{E}$ = 2 V/Å

Li O Li$_{(se)}$ Ti Li$_{(s)}$

Li-O bond formation increases with field

Ti-O bond breaking as the field increases

—0.0 V/Å —0.5 V/Å
—1.0 V/Å —2.0 V/Å
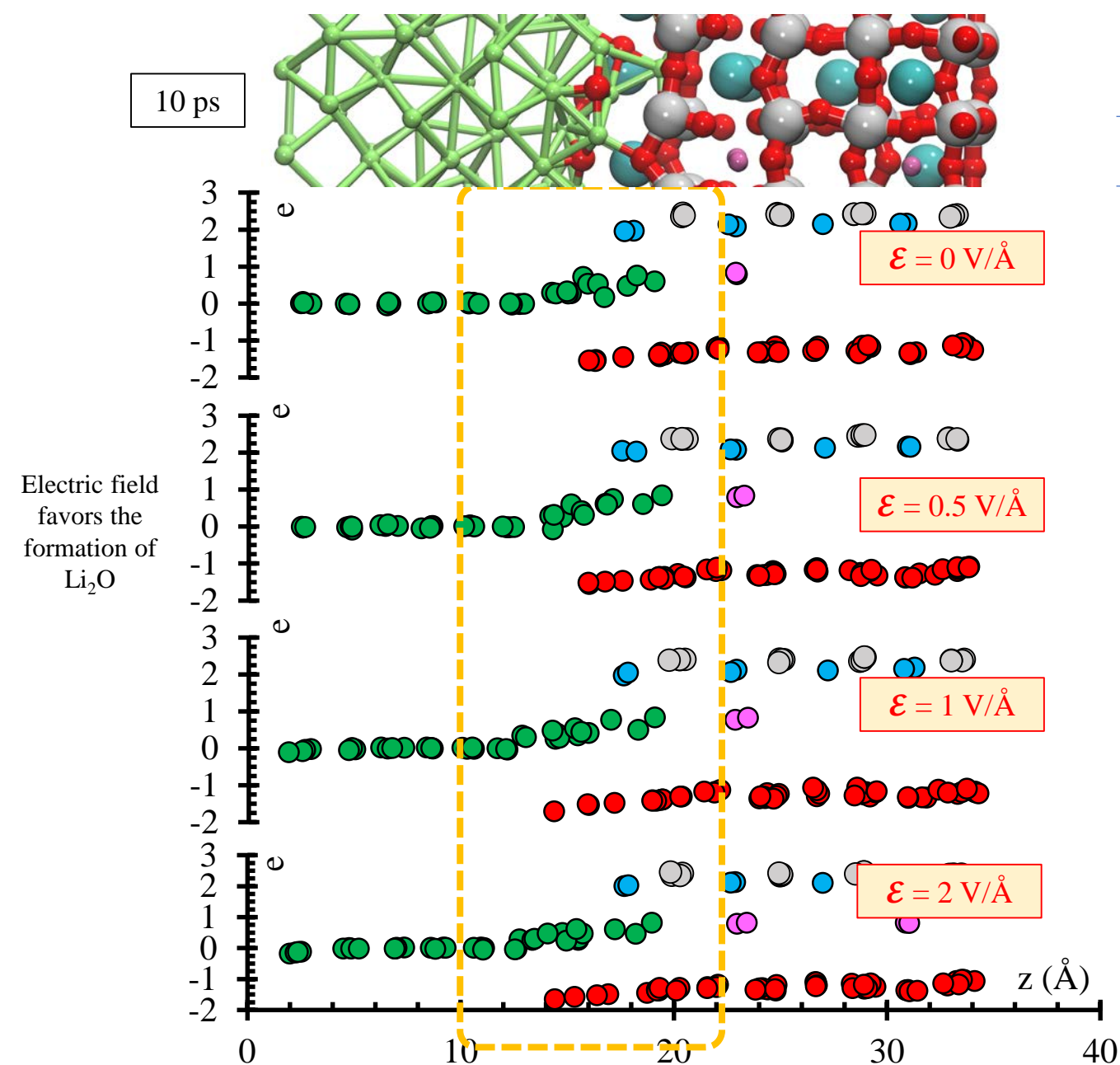
Nano-battery model: Neural Network for the conductivity calculation
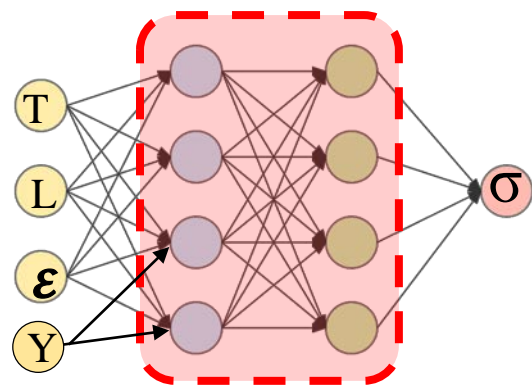
mono-physics model $\sigma_{(\varepsilon,T,L,A)}$

4 input parameters are considered to extrapolate a realistic value of the conductivity.
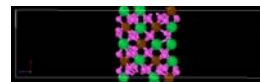
E[V/m]	T(K)	[S/cm]	L(m)	A(m2)
5E+09	290	0	1.08E-09	1.17E-18
7.5E+09	320	0.456064	1.08E-09	1.17E-18
1E+10	357	0.533595	1.08E-09	1.17E-18
1.5E+10	497	1.003341	1.08E-09	1.17E-18
2E+10	611	1.340829	1.08E-09	1.17E-18
5E+09	339	0.478867	1.08E-09	2.34E-18
7.5E+09	360	0.483428	1.08E-09	2.34E-18
1E+10	386	0.519913	1.08E-09	2.34E-18
1.5E+10	551	0.989659	1.08E-09	2.34E-18
2E+10	748	1.289522	1.08E-09	2.34E-18
5E+09	335	0.430981	1.08E-09	4.68E-18
7.5E+09	358	0.42414	1.08E-09	4.68E-18
1E+10	412	0.643051	1.08E-09	4.68E-18
1.5E+10	574	0.937212	1.08E-09	4.68E-18
2E+10	859	1.174414	1.08E-09	4.68E-18
1.5E+10	475	0.939492	1.08E-09	1.17E-18
2E+10	479	0.848279	1.08E-09	1.17E-18
5E+09	317	0.273639	1.08E-09	1.17E-18
7.5E+09	340	1.021584	1.08E-09	1.17E-18
1E+10	433	1.272419	1.08E-09	1.17E-18
1.5E+10	523	1.468527	1.08E-09	1.17E-18
2E+10	935	2.756908	1.08E-09	1.17E-18
3396.226	300	?		0.00106	0.032809

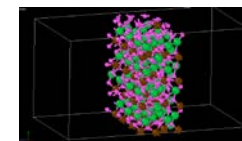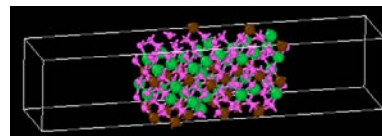| E		E[V/m]	T(K)	t[s]	Q [C]	I=Q/t [A=C/s]	J [A/m2]	[S/cm]	L(m)	A(m2)
0.5	V/A	5000000000	290	1.00E-11	0.00E+00	0.00E+00	0.00E+00	0.00000	1.0814E-09	1.16943E-18
0.75	V/A	7500000000	320	1.00E-11	4.00E-18	4.00E-07	3.42E+11	0.45606	1.0814E-09	1.16943E-18
1	V/A	10000000000	357	1.00E-11	6.24E-18	6.24E-07	5.34E+11	0.53360	1.0814E-09	1.16943E-18
1.5	V/A	15000000000	497	1.00E-11	1.76E-17	1.76E-06	1.51E+12	1.00334	1.0814E-09	1.16943E-18
2	V/A	20000000000	611	1.00E-11	3.14E-17	3.14E-06	2.68E+12	1.34083	1.0814E-09	1.16943E-18
0.5	V/A	5000000000	339	1.00E-11	5.60E-18	5.60E-07	2.39E+11	0.47887	1.0814E-09	2.33885E-18
0.75	V/A	7500000000	360	1.00E-11	8.48E-18	8.48E-07	3.63E+11	0.48343	1.0814E-09	2.33885E-18
1	V/A	10000000000	386	1.00E-11	1.22E-17	1.22E-06	5.20E+11	0.51991	1.0814E-09	2.33885E-18
1.5	V/A	15000000000	551	1.00E-11	3.47E-17	3.47E-06	1.48E+12	0.98966	1.0814E-09	2.33885E-18
2	V/A	20000000000	748	1.00E-11	6.03E-17	6.03E-06	2.58E+12	1.28952	1.0814E-09	2.33885E-18
0.5	V/A	5000000000	335	1.00E-11	1.01E-17	1.01E-06	2.15E+11	0.43098	1.0814E-09	4.6777E-18
0.75	V/A	7500000000	358	1.00E-11	1.49E-17	1.49E-06	3.18E+11	0.42414	1.0814E-09	4.6777E-18
1	V/A	10000000000	412	1.00E-11	3.01E-17	3.01E-06	6.43E+11	0.64305	1.0814E-09	4.6777E-18
1.5	V/A	15000000000	574	1.00E-11	6.58E-17	6.58E-06	1.41E+12	0.93721	1.0814E-09	4.6777E-18
2	V/A	20000000000	859	9.79E-12	1.08E-16	1.10E-05	2.35E+12	1.17441	1.0814E-09	4.6777E-18
0.5	V/A	5000000000		1.00E-11	2.72E-18	2.72E-07	2.33E+11		1.0814E-09	1.16943E-18
0.75	V/A	7500000000		1.00E-11	2.08E-18	2.08E-07	1.78E+11		1.0814E-09	1.16943E-18
1	V/A	10000000000		1.00E-11	3.68E-18	3.68E-07	3.15E+11		1.0814E-09	1.16943E-18
1.5	V/A	15000000000	475	1.00E-11	1.65E-17	1.65E-06	1.41E+12	0.93949	1.0814E-09	1.16943E-18
2	V/A	20000000000	479	1.00E-11	1.98E-17	1.98E-06	1.70E+12	0.84828	1.0814E-09	1.16943E-18
0.5	V/A	5000000000	317	1.00E-11	1.60E-18	1.60E-07	1.37E+11	0.27364	1.0814E-09	1.16943E-18
0.75	V/A	7500000000	340	1.00E-11	8.96E-18	8.96E-07	7.66E+11	1.02158	1.0814E-09	1.16943E-18
1	V/A	10000000000	433	1.00E-11	1.49E-17	1.49E-06	1.27E+12	1.27242	1.0814E-09	1.16943E-18
1.5	V/A	15000000000	523	1.00E-11	2.58E-17	2.58E-06	2.20E+12	1.46853	1.0814E-09	1.16943E-18
2	V/A	20000000000	935	1.00E-11	6.45E-17	6.45E-06	5.51E+12	2.75691	1.0814E-09	1.16943E-18

L / A$_t$

L / 2A$_t$

L / 4A$_t$

2 L / A$_t$

4 L / A$_t$

NN result At 300 K → σ = 0.00031 S/cm

Experimental At 300 K → σ = 0.00023 S/cm